Drug Development and Industrial Pharmacy, 2011, 37(3): 290–299

ISSN 0363-9045 print/ISSN 1520-5762 online
DOI:10.3109/03639045.2010.510141

informa
healthcare

ORIGINAL ARTICLE

Effect of (E)-2-isopropyl-5-methylcyclohexyl octadec-9-enoate on transdermal delivery of *Aconitum* alkaloids

Ligang Zhao[1,2], Liang Fang[1], Yan Li[1,2], Ni Zheng[1], Yongnan Xu[1], Jinghua Wang[1] and Zhonggui He[1]

[1]*Department of Pharmaceutical Sciences, Shenyang Pharmaceutical University, Shenyang, Liaoning, China and* [2]*Institute of Pharmaceutical Sciences, QILU Pharmaceutical Co., Ltd., Jinan, Shandong, China*

Abstract

Objective: The aim of this work was to evaluate the percutaneous absorption of *Aconitum* alkaloids using (*E*)-2-isopropyl-5-methylcyclohexyl octadec-9-enoate (M-OA) as an enhancer as well as to investigate the effect of M-OA in isopropyl palmitate (IPP) solution (5% ethanol in IPP, w/v), with or without an enhancer, on the stratum corneum (SC) barrier properties in vitro. *Methods*: The in vitro permeation studies of *Aconitum* alkaloids were conducted in isopropyl myristate (IPM) solution in side-by-side diffusion cells. In addition, scanning electron microscopy (SEM) and attenuated total reflectance Fourier transform infrared (ATR-FTIR) spectroscopy were used to evaluate the M-OA biophysical changes in SC barrier function in vitro. *Results*: The in vitro permeation studies indicated that M-OA had significant enhancing effect on the permeation of mesaconitine (MA) and hypaconitine (HA); however, aconitine (AC) was too low to be detected on the receiver side, and L-menthol had no effect on the penetration of all the *Aconitum* alkaloids. Morphological changes in the skin after enhancer treatment demonstrated that the extraction of the SC lipids by the enhancers led to disruption of the SC and the desquamation of SC flake. ATR-FTIR spectra of C–H asymmetric/symmetric stretching peak shifts and amide II stretching vibrations were indicative of SC lipid fluidization and changes in protein conformation, respectively. *Conclusion*: The results showed that M-OA was worthy of further investigation as a potential candidate for inclusion in transdermal formulations as a penetration enhancer.

Key words: *Aconitum* alkaloids, ATR-FTIR, L-menthol, oleic acid, SEM

Introduction

Plants of the genus *Aconitum* (Ranunculaceae), including Chuanwu (*Aconitum carmichaelii* Debx.), Caowu (*Aconitum kusnezoffii* Reichb.), and Fuzi (A. carmichaelii Debx.), are widely distributed across Asia and North America. Diesterditerpene-type *Aconitum* alkaloids (presented in Figure 1), such as aconitine (AC), mesaconitine (MA), and hypaconitine (HA), are widely used in both China and Japan for the treatment of the common cold, polyarthralgia (such as rheumatoid arthritis), skin wounds, depression, diarrhea, and heart failure[1,2]. However, owing to their high toxicity, the oral administration of *Aconitum* alkaloids is often limited on account of dose-related adverse side effects, including palpitations, chest tightness, hypotension, nausea, abdominal pain, and diarrhea[2]. *Aconitum* alkaloids are extensively metabolized following oral administration, and their major metabolites act in a similar fashion as the parent compound on receptors[3], which restricts their application in patients with liver cirrhosis. In addition, the oral route of drug delivery is not preferable for patients with severe nausea; also, the short elimination half-life of *Aconitum* alkaloids requires frequent dosing. Hence, the transdermal route could be a better alternative route for these patients, because it bypasses first-pass metabolism, minimizes the gastrointestinal side effects, increases patient compliance, maintains a constant drug level in plasma, and makes it possible to interrupt or terminate treatment when necessary (which is especially important for a drug with high toxicity)[4]. However, there is no literature report on the skin permeation of *Aconitum* alkaloids either in vitro or in vivo. An essential prerequisite for the development of a transdermal drug delivery system (TDDS) is that the

Address for correspondence: Dr. Liang Fang, Department of Pharmaceutical Sciences, Shenyang Pharmaceutical University, 103 Wenhua Road, Shenhe District, Shenyang, Liaoning 110016, China. Tel: +86 24 23986330, Fax: +86 24 23986330. E-mail: fangliang2003@yahoo.com

(Received 24 Oct 2009; accepted 17 Jul 2010)

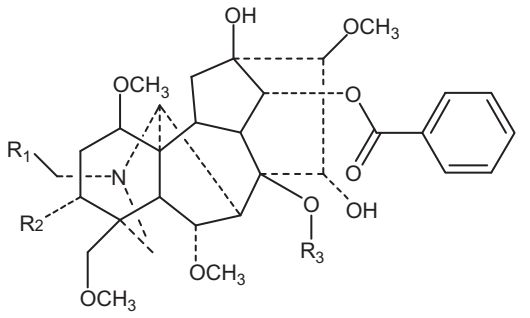

Name	R_1	R_2	R_3
AC	CH_3	OH	Acetyl
MA	H	OH	Acetyl
HA	H	H	Acetyl

Figure 1. The chemical structures of *Aconitum* alkaloids (including AC, MA, and HA).

drug must be capable of passing through the skin at a sufficiently high rate to achieve therapeutic plasma concentrations. However, the outermost layer of skin, the stratum corneum (SC), forms a major barrier to most exogenous substances, including drugs[5]. One popular approach to deliver an effective dose of drug through skin is to reversibly reduce the barrier function of the skin with the aid of penetration enhancers or accelerants[6]. More recently, new types of O-acylmenthol derivatives have been synthesized in our laboratory and their promoting activities have been evaluated using model drugs with a range of lipophilicity[7,8]. According to the penetration results both from patch in vitro and from permeation studies in rats in vivo, (*E*)-2-isopropyl-5-methylcyclohexyl octadec-9-enoate (M-OA) (shown in Figure 2) exhibited good in vitro/in vivo penetration activity for tolterodine[9], which would be important for its application to enhance the penetration of *Aconitum* alkaloids in this study. Moreover, as esterases are present in the human and animal epidermis[10], the ester linkage of M-OA offers the possibility of degradation by skin esterases in the living epidermis that would increase enhancer safety. To further evaluate the effectiveness of M-OA in vitro, the parent compound L-menthol was also used as a reference-enhancing promoter.

Biophysical evidence on the extent and duration of the effect of an enhancer can be provided through

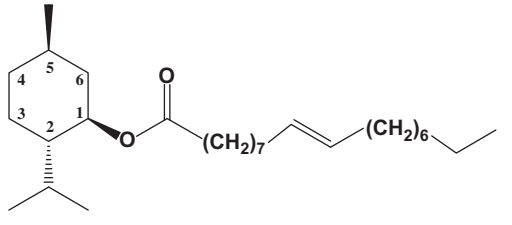

Figure 2. The chemical structure of M-OA.

measurements using scanning electron microscopy (SEM) and attenuated total reflectance Fourier transform infrared (ATR-FTIR) spectroscopy. SEM has been shown to be useful in assessing macroscopic changes in the functional state of the skin barrier and contributes to the prediction of percutaneous penetration[11,12]. However, ATR-FTIR allows conformational changes in SC lipid and protein domains to be detected, and has proved to be a useful tool for monitoring the percutaneous penetration of drugs or other constituents such as cosolvents and enhancers[13–15]. In addition, ATR-FTIR also shares the advantage of being noninvasive and enabling experiments to be conducted in vitro and in vivo[16–18]. The probe-free and noninvasive technique ensures that the experimentally obtained vibrations directly reflect the characteristics of the SC. Using ATR-FTIR, it is thought to be possible to observe the lipid organization in the SC not only on the surface, but also in deeper regions in the SC[19].

The purpose of this investigation was to evaluate the influence of M-OA on the transdermal delivery of *Aconitum* alkaloids through the abdominal skin of rats, and we further analyzed the penetration mechanism by which M-OA interacted with the lipid and protein of the porcine skin SC, using SEM and ATR-FTIR in vitro.

Materials and methods

Materials

Standards of AC, HA, and MA were purchased from the Chinese Authenticating Institute of Material and Biological Products (Beijing, China); *Aconitum* alkaloid mixtures that contain 7.45% AC, 21.46% MA, and 52.16% HA (w/w) were kindly provided by the College of Chinese Traditional Medicine, Shenyang Pharmaceutical University; isopropyl myristate (IPM), isopropyl palmitate (IPP), and L-menthol were purchased from China National Medicines Co., Ltd. (Shanghai, China); M-OA was synthesized as described in previous reports[7], and its structure was confirmed by NMR (ARX-300, Bruker, Switzerland) and high-performance liquid chromatography–mass spectrometry (HPLC-MS) (ZQ-2000, Waters, Milford, CT, USA); acetonitrile of HPLC grade was obtained from the Yuwang Pharmaceutical Co., Ltd. (Shandong, China). All other chemicals were of the highest reagent grade available.

Drug analysis

The HPLC system for analyzing drug concentrations was equipped with an L-2420 variable-wavelength ultraviolet absorbance detector and an L-2130 pump (Hitachi High-Technologies Corporation, Tokyo, Japan). The reversed phase stainless steel column (200 mm × 4.6 mm) was packed with Diamonsil C-18 (5 μm particle size; Dikma Technologies, Beijing, China). The mobile phase for the *Aconitum* alkaloids consisted of acetonitrile and 0.2% acetic acid in distilled water (32:68, v/v), the pH

was adjusted to 6.25 with triethylamine, the flow rate was 1.0 mL/min, detection was carried out at 240 nm, and an external calibration method was used. The retention times of the three *Aconitum* alkaloids were 21.10, 24.68, and 30.48 minutes for MA, AC, and HA, respectively.

Solubility determination

To determine the saturation solubility of the *Aconitum* alkaloids in IPM, with and without enhancers, 30 mg mixture (1.5% mixture, w/v) was added into 2 mL vehicle, vortexed for 2 minutes followed by sonication for 10 minutes to dissolve the drug and then equilibrated at 32 ± 0.5°C for more than 48 hours. Finally, the suspensions were filtered through a 0.45-μm membrane filter and the supernatant saturated solution was diluted with mobile phase for 25 times and analyzed using HPLC. The experiments were performed in triplicate.

Partition coefficients determination

n-Octanol and water were mutually saturated for 24 hours before the experiment. The solution (200 μg/mL) of AC, MA, and HA was prepared using *n*-octanol saturated with water. One milliliter of the solution was then transferred to a 10-mL centrifuge tube containing 1 mL of water saturated with *n*-octanol. The tube was gently shaken for 48 hours at 25 ± 0.5°C and centrifuged at 8600 × g for 10 minutes. After centrifugation, the AC, MA, and HA concentrations in each phase were determined using a validated HPLC method.

Enhancer-containing solutions preparation

Control solution was obtained by equilibration of 5% (w/w) ethanol in IPP; enhancer-containing solutions were prepared by equilibration of selected amounts of L-menthol (5%, w/w) or M-OA (13.5%, w/w) in control solution, then vortexed for 2 minutes followed by sonication for 10 minutes to dissolve the enhancer. The molar concentration of the M-OA in this study was the same as the concentration of L-menthol, which was 5% (w/w).

Skin preparation for ATR-FTIR

Pig ears were obtained from a slaughterhouse, and the dorsal fur of the ear was removed carefully with 0.1-mm hair clippers. The skin was carefully excised, and any skin with a disrupted barrier was removed. The skin was cut to a size of about 2 cm × 2 cm. For ATR-FTIR studies, the epidermis membranes were prepared by heat separation[20]; excess subcutaneous fat and connective tissue were removed from the skin, which was then immersed in water at 60°C for 45 seconds. The epidermal membrane was gently teased off and floated SC side up overnight at 37 ± 0.5°C on a pH 7.4 phosphate-buffered saline (PBS) solution of trypsin (0.25%, w/v). The digested epidermal remnants were removed by swabbing. The SC membranes were washed with distilled water and then dried in a vacuum drying oven until required.

ATR-FTIR spectroscopy study

FTIR spectra were recorded using a Magna-8300 spectrophotometer (Nicolet, Madison, WI, USA) equipped with a Ge IRE (with a 45° incident angle). Each measurement represented an average of 200 scans with a resolution of 4 cm^{-1} from 1000 to 4000 cm^{-1}. Location of the IR absorbance-peak maximum was determined to an accuracy of 0.1 cm^{-1} using origin 7.0 (a software). To determine the lipid fluidization effect of the M-OA, the frequencies of the peaks assigned to the CH_2 symmetric/asymmetric stretching vibrations of the SC lipid alkyl chains was studied; an interaction with skin proteins was also investigated by analysis of changes in the amides I/II stretching vibration in the recorded spectra. The SC was incubated in control solution, permeation enhancer solution (5% (w/w) L-menthol or 13.5% (w/w) M-OA in control solution) for 12 hours at ambient temperature and washed three times with purified water, then dried with tissue paper, finally dried under a stream of nitrogen for 48 hours.

SEM ultrastructural examination

Excised porcine epidermis samples were cut into appropriate size cubes and treated with control solution, L-menthol, or M-OA solution for 12 hours at room temperature, then washed six times with ethanol and immediately fixed in 2.5% glutaraldehyde buffer solution overnight, washed three times with 0.2 M cacodylate and 7% sucrose buffer for 15 minutes post-fixed with 2% osmium tetroxide for 1 hour, washed three times as above, and immersed in 0.5% aqueous uranyl acetate for 30 minutes. Specimens were then dehydrated in graded concentrations of ethanol, transferred to isoamyl acetate, and critical point dried using liquid carbon dioxide. The dried specimens were affixed with gold–palladium in an ion coater and examined with a SEM (Hitachi S-3005N, Tokyo Japan). All histopathologic analyses were performed in a blinded fashion.

Permeation experiments

Donor solutions of the *Aconitum* alkaloids were obtained by equilibration of excess amounts of solute in donor solvent (1.5% mixture, w/v), which were much higher than the solubility of solute in donor solvent, then vortexed for 2 minutes followed by sonication for 10 minutes to dissolve the drug. The molar concentration of the M-OA in this study was the same as the molar concentration of L-menthol; the mass concentration of L-menthol and M-OA were 5% and 13.5% (w/w), respectively; an excess amount of solute was present throughout the experiments.

Male Wistar rats weighing 180–220 g (6–8 weeks old) used in all experiments were supplied by the Experimental Animal Center of Shenyang Pharmaceutical University (Shenyang, China). The experiments were performed in accordance with the guidelines for animal use published by the Life Science Research Center of Shenyang

Pharmaceutical University. The rats were anesthetized with urethane (20%, w/v, i.p.) and the abdomen was carefully shaved with a razor after removal of hair by electric clippers (model 900, TGC, Hokkaido, Japan). Full thickness skin (i.e., epidermis with SC and dermis) was excised from the shaved abdominal site. The integrity of the skin was carefully checked under the microscope, and any skin that was not uniform was rejected. After removing the fat and subdermal tissue, the skin was kept frozen at −20°C and used within 1 week. Before starting the experiments, the skin was allowed to reach room temperature for at least 10 hours.

Skin permeation experiments were performed according to the method of Fang et al.[21] A diffusion cell consisting of two half-cells with a water jacket connected to a water bath at 32°C was used. Each half-cell had a volume of 2.5 mL and an effective area of 0.95 cm^2. The dermis side of the skin was in contact with the receiver compartment and the SC with the donor compartment. The donor compartment was filled with the drug suspension and the receiver compartment with pH 7.4 PBS. During all the experiments, excess drug was maintained in the donor compartment. Both donor and receiver compartments were stirred with a star-head bar driven by a constant speed synchronous motor at 600 rpm. At predetermined time intervals, 2.0 mL of the receptor solution was withdrawn from each receiver compartment for analysis and replaced with the same volume of fresh solution to maintain sink conditions.

Data analysis

The cumulative amount of drugs permeating through the skin was plotted as a function of time. The skin flux was determined from Fick's law of diffusion:

$$J_s = \frac{dQ_r}{A\,dt}$$

where J_s is the steady-state skin flux in μg/cm^2/h, dQ_r is the change in quantity of the drug passing through the skin into the receptor compartment in μg, A is the active diffusion area in cm^2, and dt is the change in time. The flux was calculated from the slope of the linear portion of the profiles[22].

The permeability coefficient (P) was calculated as described in Scheuplein[23].

$$P = \frac{J_s}{C_s},$$

where C_s is the saturated solubility of drugs in donor solutions.

All parameters were reported as the mean ± SE. Statistical analysis was carried out using analysis of variance (ANOVA). The level of significance was taken as $P < 0.05$.

Results and discussion

In vitro permeation of *Aconitum* alkaloids

The partition coefficients (log $K_{O/W}$) for MA, HA, and AC were listed in Table 1. Table 2 shows the permeation parameters of MA and HA that permeated through the rat skin; however, the concentration of AC in the receptor phase was too low to be detected in the permeation experiment. Between the enhancer examined, M-OA had a significant enhancing effect on the permeation of MA and HA through the skin, whereas L-menthol had no promoting effect ($P > 0.05$) on the permeation of all the Aconitum alkaloids, as shown in Figure 3. The solubility parameter of M-OA was similar to that of IPM[7], which ensured that M-OA is fully compatible in IPM and, so, the mixture of M-OA and IPM could be delivered to the SC. When using IPM, a known fluidizer of intercellular lipids[24,25], as a vehicle, the enhancing activity of O-acylmenthol derivatives for TOL was relatively low (ER values < 5), and this was also observed in this study. The addition of M-OA had a greater enhancing effect on the skin permeation of MA and HA, and this result agreed well with our previous reports that investigated the effects of M-OA on lipophilic and hydrophilic drugs[8,9]. Indeed, experimental verification of hypothesis that distinct hydrophilic (polar) and lipophilic (nonpolar) pathways exist for hydrophilic and hydrophobic drugs has come from the work by Yamashita et al.[26,27] who analyzed the skin permeation of drugs based on a two-layer model with polar and nonpolar routes in the SC and found that the action of permeation enhancers could be described in terms of the drug diffusivity and partition coefficient in each domain. M-OA has a high hydrophobicity and viscosity, which could contribute to the more pronounced effect on nonpolar pathways, which involved the esterified fatty acids within the SC that contributes to diffusional resistance[28].

Skin morphology study

Morphological changes in the skin surface treated with control solution or enhancer-containing solution were examined using SEM (presented in Figure 4), which showed typical examples of microscopic images of the skin surface treated with IPP solution, with or without enhancer, for 12 hours. The micrograph of the untreated epidermis at ×500 magnification (Figure 4a) showed a

Table 1. The partition coefficients (log $K_{O/W}$) for AC, MA, and HA.

Compounds	log $K_{O/W}$
AC	0.67
MA	0.64
HA	0.85

Table 2. Skin permeation rates of MA and HA through rat abdominal skin. The donor phases consisted of IPM; IPM: menthol (20: 1) (w/w) and an equivalent molar amount of M-OA with L-menthol in IPM.

Enhancers	Permeants	Solubility (μg/mL)	J_{ss} (μg/cm^2/h)	P (cm/h) ×10^3	T_{lag} (h)	ER[a]
Control	MA	251.05	0.49 ± 0.10	1.97 ± 0.41	0.71	1.00
	HA	467.99	0.45 ± 0.10	0.97 ± 0.21	0.51	1.00
L-Menthol	MA	202.26	036 ± 0.03	1.78 ± 0.15	0	0.85
	HA	328.44	0.39 ± 0.05	1.18 ± 0.14	0	0.91
M-OA	MA	161.47	0.86 ± 0.11*	5.31 ± 0.70*	3.26*	1.34*
	HA	207.69	0.86 ± 0.11*	4.13 ± 0.54*	4.92*	1.62*

*Value is significantly different from control ($P < 0.05$). [a]ER is the enhancement ratio calculated as follows: ER = Q (with enhancer)/Q (without enhancer). Data are given as average ± SD (n = 4).

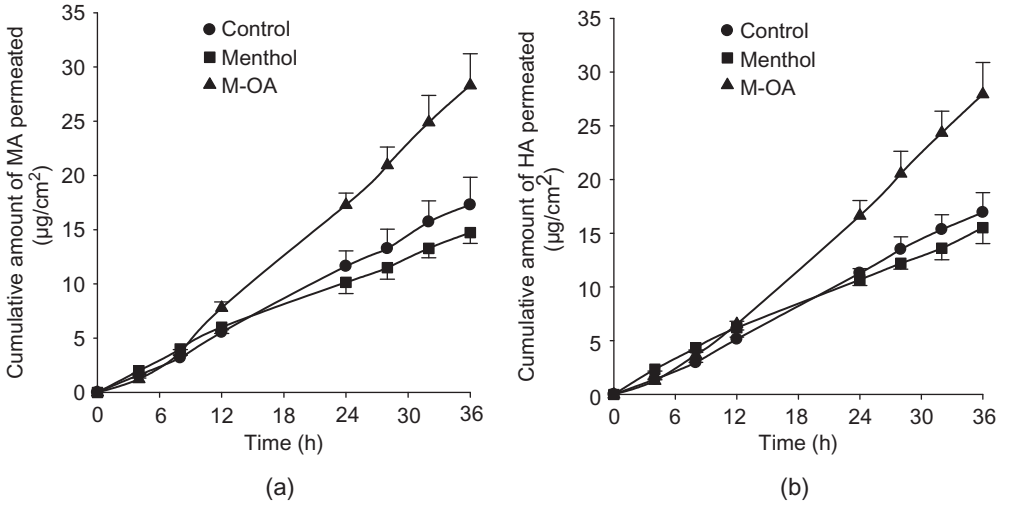

Figure 3. Permeation profiles of drugs through rat skin (average ± SE, n = 4): (a) MA; (b) HA.

closely united assembly of squamous cells, with a ridge and furrow pattern. The cells show irregular folds, convolutions, and occasionally, a villous appearance. Cell margins are difficult to see as adjacent cells appear to merge because of their close apposition. These cells enclose keratin filaments embedded in an amorphous matrix of mainly lipid and non-fibrous protein. The SEM images of skin treated with control solution (Figure 4b) showed significant modification of the skin surface. There were many cavities present on the surface of skin and the intercellular space is slightly distended, but there was no desquamated SC flakes in the intact skin of the control, suggesting that the extraction of intercellular lipids bilayers by the control solution was slightly. As shown in Figure 4c, the skin surface following L-menthol treatment was eroded and appeared rougher than that of the group treated with control solution. It was observed that a large number of flakes were desquamated from the intact porcine skin treated with L-menthol and the cavities on the skin surface were larger than those of the control group. The most marked changes in the skin surface were found with the M-OA treatment (Figure 4d). It was found that the junctions between the cells had become extremely loose and the cell separation had increased considerably resulting in very large intercellular spaces, which suggested a decrease in the barrier resistance of SC after treatment by the M-OA. In addition, the numerous cavities present on the surface of the skin after M-OA treatment were attributed to lipid extraction of the skin resulting in an increase in drug permeation. In general, morphological alterations of the skin structure increased in the order of the blank group < control group < menthol < M-OA. The SC is composed of corneocytes enclosed by a continuous intercellular lipid domain[29,30]. When the porcine skin was dipped in the enhancer solution, the intercellular lipid was probably dissolved and extracted by the solution, leading to the corneocytes separating from each other. This is probably the reason that the SC flake desquamates from the intact SC. The results demonstrated that the permeation mechanism of the enhancers involved extracting SC lipids and the extract lipid action of M-OA was more potent than that of L-menthol and control solutions.

In determining the penetration effect of L-menthol and M-OA on the SC of the skin, IPP was employed as the vehicle because of the solubility parameters of M-OA and L-menthol being similar to that of IPP, which ensured that M-OA and L-menthol were fully compatible in IPP, and, so, the mixture of M-OA/L-menthol and IPP could be delivered effectively to the SC. In addition,

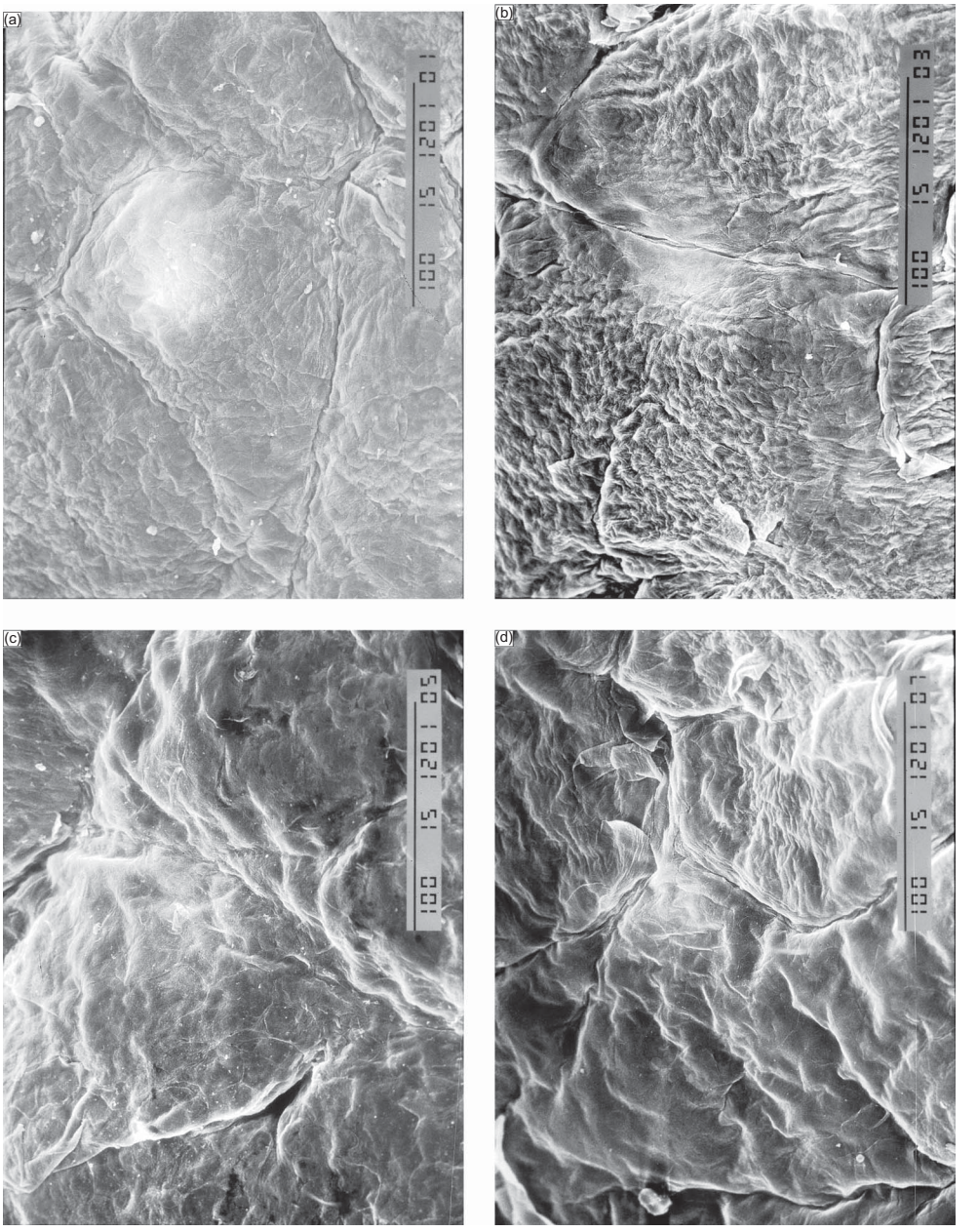

Figure 4. Scanning electron micrographs (×500) of porcine skin SC treated with solution, with or without enhancer. The SC was photographed after 12 hours of exposure to the solutions and standard treatment. (a) The blank skin surface showed a rough morphology, (b) After the control solution treatment, the roughness of the skin surface was increased, (c) The skin surface was eroded and appeared rougher than control treated with L-menthol solution; and (d) The junctions between the cells have become loose, and numerous cavities are present on the skin surface following treatment with M-OA solution.

as IPP was regarded as a solvent having no enhancing effect, only few reports can be found confirming its penetration-enhancing capacity[31,32]. It is well known that ethanol is a skin penetration enhancer that affects the SC. Ethanol, at a concentration higher than 10%, has the ability to accelerate the skin penetration of a variety of substances mainly because it interacts with intercellular lipid domains of the SC, and delaminates the horny layer[33,34]. In addition, a 'drag-pull' effect observed by Fang et al.[35] could also facilitate the permeation of the solute. Also, ethanol is a relatively polar solvent that has the ability to penetrate rapidly into skin accompanied by the compound dissolved in it, just as literature reported[19]. The concentration of ethanol at 5% in IPP may facilitate partitioning of the L-menthol and M-OA from the IPP into the porcine skin; by this way more clear SEM photos could be obtained. However, as ethanol was found to be an active enhancer, the amount of ethanol in IPP should be kept low to avoid the promoting effect of ethanol exceeding the effect of L-menthol and M-OA.

ATR-FTIR studies

The light of ATR-FTIR can attain approximately 1 μm in depth at specific area. Moreover, the distribution of components are thought to be heterogeneous in SC. Thus, the change in infrared spectra derived from lipids at the surface of SC gave authors the useful information of intercellular lipids affected by the administration of absorption enhancers. ATR-FTIR spectral shifts of porcine SC treated with enhancers are shown in Table 3. Representative IR absorbance spectra from 4000 to 2600 and 2200 to 1200 cm^{-1} of changes in the C–H stretching region and the amide band after treatment of SC with IPP solution, with or without enhancer, are displayed in Figures 5 and 6. The results showed that the SC treated with enhancers produced a higher shift in asymmetric/symmetric C–H vibration peak positions (around 2920 and 2850 cm^{-1}) and a lower shift in the stretching vibration peak position of amide II (plane bending mode νNH, around 1540 cm^{-1}). The peak shifts produced by

Table 3. Changes in ν_{as}/ν_s (C–H) and amides I/II stretching absorbance peaks of porcine SC after treatment with control solution or enhancer solution.

Treatments	ν_{as} (C–H)	ν_s (C–H)	Amides I	Amides II
Control	0.2 ± 0.05	0.2 ± 0.06	0.1 ± 0.05	0.1 ± 0.03
L-Menthol	1.2 ± 0.5	1.1 ± 0.5	0	1.0 ± 0.4
M-OA	1.7 ± 0.5	1.8 ± 0.6	0.1 ± 0.03	1.5 ± 0.6

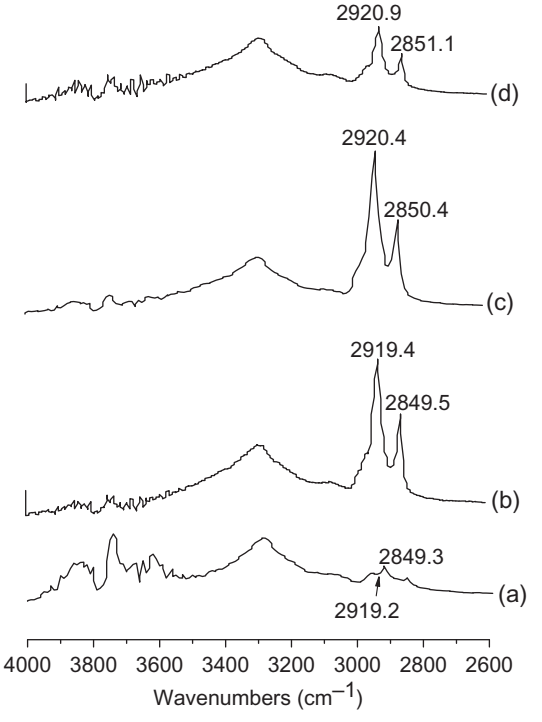

Figure 5. ATR-FTIR spectra of the porcine SC showing asymmetric and symmetric C–H bond stretching absorbance before and after enhancer treatment: (a) no treatment; (b) treated with control solution; (c) treated with L-menthol solution; and (d) treated with M-OA solution.

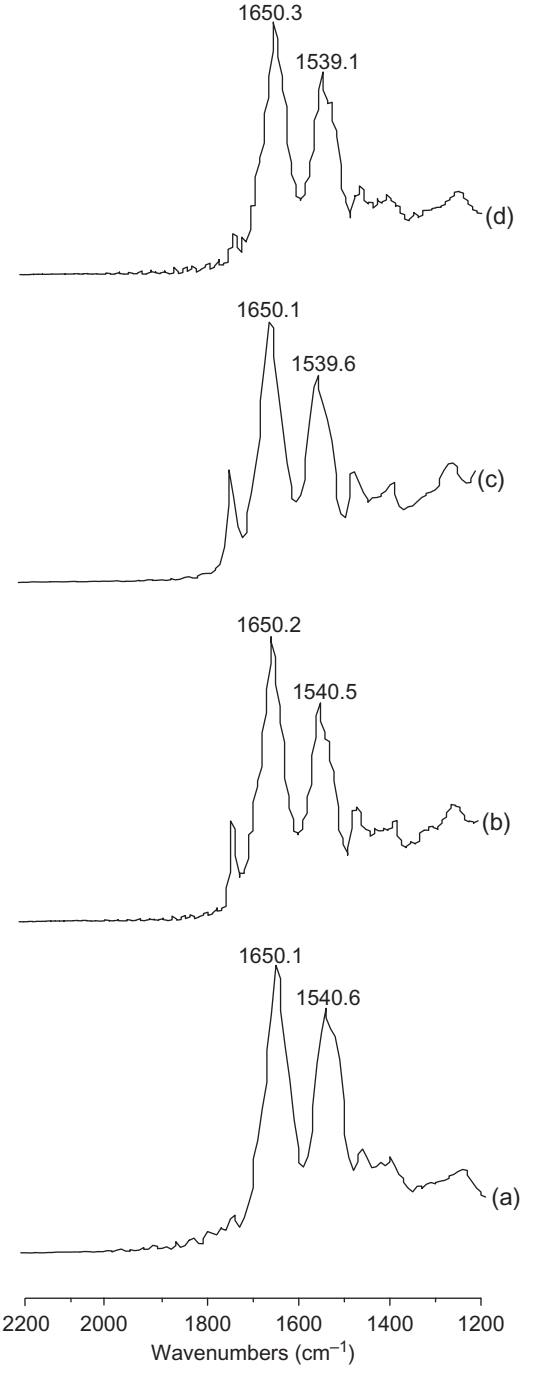

Figure 6. ATR-FTIR spectra representing amides I and II of the porcine SC before and after enhancer treatment: (a) no treatment; (b) treated with control solution; (c) treated with L-menthol solution; and (d) treated with M-OA solution.

control solution, L-menthol, and M-OA in $\nu_a(CH_2)$ were 0.2, 1.2, and 1.7 cm^{-1} and in $\nu_{as}(CH_2)$ absorption were 0.2, 1.1, and 1.8 cm^{-1}, in comparison with that of blank. The $\nu_a(CH_2)$ and $\nu_{as}(CH_2)$ peak shifts by M-OA were higher than that of L-menthol, and there were only very minor changes in $\nu_a(CH_2)$ and $\nu_{as}(CH_2)$ after control solution treatment; this phenomenon may be explained by lipid extraction or loss of lipid disorder produced by

ethanol[19]. There were no obvious peak shifts of amide I (carbonyl stretch νC=O in the CO–NH group, around 1650 cm^{-1}) before and after the enhancer treatment, and the decrease in the peak position of amide II stretching vibration is given in Table 3, this phenomenon was consistent with previous reports[36]. The peak shifts in the stretching vibration of amide II by control, L-menthol, and M-OA solutions compared with blank were 0.1, 1.0, and 1.5 cm^{-1}, respectively. In addition, there were no significant differences ($P > 0.05$) in the stretching vibration of amide II between blank and control group. These results suggest that in case of M-OA and L-menthol, the externally applied enhancers can disrupt the SC lipid structure, whereas in case of control solution, the ethanol could slightly increase the rotational of lipid acyl chains leading to increased fluidity of skin lipids, as observed by Dubey[37]. The amide II absorption peaks are the main indices to evaluate the secondary structure of keratin in SC. Using the blank absorption peak as a benchmark, the displacement of the amide II absorption peak to lower wavelength was examined to suggest the changes of keratin structure under the effect of enhancers[38–40].

ATR-FTIR had been used to investigate the biophysical changes of properties in the lipid bilayer. A representative ATR-FTIR spectrum of porcine skin SC exhibited an absorption peak of C–H bending vibration and stretching vibration from the free fatty acid in lipids. The C–H bending vibration was much weaker than the C–H stretching vibration[41]. Thus, the study of lipid biophysical changes showed that the peaks near 2920 and 2850 cm^{-1} were produced by the asymmetric and symmetric C–H stretching absorption[42–45]. Casal and Mantsch have explained the shift in C–H stretching absorption at a molecular level[46]. The shift to higher frequency occurred when CH_2 groups along the alkyl chain of lipids changed from trans to gauche conformation, and indicated that the SC lipid was perturbed. The lipids are thus thought to exist in a more fluid-like state and this is termed the liquid crystalline phase. The magnitude of the shift in C–H stretching vibration was directly related to the ratio of trans to gauche conformers in the alkyl chain. The higher the shifts, the higher the ratio of trans to gauche. It was demonstrated that the promoters causing the higher shift of C–H stretching vibration improved drug permeation[14,47–49]. The higher the shift of C–H stretching vibration produced, the stronger the ability to perturb the SC lipids. It can be concluded that the ability of M-OA to disorder the SC lipids was more potent than that of L-menthol and control solution. The enhancement mechanism of M-OA included a disorder of the SC lipids to a different extent. The spectral shift of C–H stretching vibration changed by M-OA was lower than that of the spectral shift reported in the literature[50,51]. These results suggest that, besides the enhancement mechanism of perturbing and extracting the SC lipids, another mechanism plays an important role in the penetration of M-OA.

M-OA may penetrate into the corneocytes and disrupt the keratin filament network, thereby rendering the corneocytes more permeable. Figure 6 compares the ATR-FTIR spectra over the range 1850–1300 cm^{-1} of untreated SC and SC treated with IPP solution, with or without enhancer. Compared with untreated sample, the amide II bands shifted reproducibly by about 1.5 cm^{-1} to lower wavenumbers after the application of IPP solution containing M-OA. A previous literature report states that the observed amide II bands in SC at about 1540 and 1508 cm^{-1} can be attributed to α-helical conformation and β-pleated sheets, respectively[52]. The changes observed in this investigation are consistent with conversion of the protein from an α-helical conformation to β-pleated sheets that has been observed in other natural proteins and synthetic polypeptides[53]. Altogether, the protein conformation change decreased the conformational integrity and increased the permeability of proteins. So, the changes outlined above suggest that increased transdermal flux of MA and HA correlates with increased SC lipid fluidization and alters the SC protein conformation caused by exposure to IPP solution with M-OA.

Conclusions

This investigation has demonstrated that the penetration of *Aconitum* alkaloids (MA, HA) is increased in the presence of M-OA used as an enhancer. It is apparent that M-OA can modify the lipid fluidity and change the protein conformation of the SC to promote the penetration of MA and HA. Overall, the action of M-OA on the lipids and keratin results in looser or more permeable structures, which are presumably responsible at least in part for the observed increases in the flux of MA and HA following M-OA treatment.

Acknowledgment

The authors thank Professor Yasunori Morimoto, Faculty of Pharmaceutical Sciences, Josai University, Japan, for providing the two-chamber diffusion cells.

Declaration of interest

The authors report no conflicts of interest. The authors alone are responsible for the content and writing of this article.

References

1. Kolev ST, Leman P, Kite GC, Stevenson PC, Shaw D, Murray VSG. (1996). Toxicity following accidental ingestion of *Aconitum* containing Chinese remedy. Hum Exp Toxicol, 15:839–42.
2. Lin CC, Chan TYK, Deng JF. (2004). Clinical features and management of herb-induced aconitine poisoning. Anal Emer Med, 43:574–79.

3. Zhang HG, Sun Y, Duan MY, Chen YJ, Zhong DF, Zhang HQ. (2005). Separation and identification of *Aconitum* alkaloids and their metabolites in human urine. Toxicon, 46:500–06.
4. Kiptoo PK, Hamad MO, Crooks PA, Stinchcomb AL. (2006). Enhancement of transdermal delivery of 6-beta-naltrexol via a codrug linked to hydroxybupropion. J Control Release, 113:137–45.
5. Hui X, Wester RC, Zhai H, Maibach HI. (2005). Chemical partitioning into powdered human stratum corneum: A useful *in vitro* model for studying interaction of chemicals and human skin. In: Bronaugh RL, Maichach HI, eds. Percutaneous absorption. Boca Raton: Taylor & Francis, 291–302.
6. Hadgraft J. (1999). Passive enhancement strategies in topical and transdermal drug delivery. Int J Pharm, 184:1–6.
7. Zhao L, Fang L, Xu Y, Liu S, He Z, Zhao Y. (2008a). Effect of *O*-acylmenthol on transdermal delivery of drugs with different lipophilicity. Int J Pharm, 352:92–103.
8. Zhao L, Fang L, Xu Y, Zhao Y, He Z. (2008b). Transdermal delivery of penetrants with differing lipophilicities using *O*-acylmenthol derivatives as penetration enhancers. Eur J Pharm Biopharm, 69:199–213.
9. Zhao L, Li Y, Fang L, He Z, Liu X, Wang L, et al. (2009). Transdermal delivery of tolterodine by *O*-acylmenthol: *In vitro*/*in vivo* correlation. Int J Pharm, 374:73–81.
10. Montagna W. (1955). Histology and cytochemistry of human skin IX. The distribution of non-specific esterases. J Biophys Biochem Cyol, 1:13–16.
11. Fang JY, Hwang TL, Leu YL. (2003). Effect of enhancers and retarders on percutaneous absorption of flurbiprofen from hydrogels. Int J Pharm, 250:313–25.
12. Zhang CF, Yang ZL, Luo JB, Zhu QH, Zhao HN. (2007). Effects of cinnamene enhancers on transdermal delivery of ligustrazine hydrochloride. Eur J Pharm Biopharm, 67:413–19.
13. Dias M, Raghavan SL, Hadgraft J. (2001). ATR-FTIR spectroscopic investigations on the effect of solvents on the permeation of benzoic acid and salicylic acid through silicone membranes. Int J Pharm, 216:51–59.
14. Levang AK, Zhao K, Singh J. (1999). Effect of ethanol/propylene glycol on the *in vitro* percutaneous absorption of aspirin, biophysical changes and the macroscopic barrier properties of the skin. Int J Pharm, 181:255–63.
15. Pellett MA, Watkinson AC, Hadgraft J, Brain KR. (1997). Comparison of permeability data from traditional diffusion cells and ATR-FTIR spectroscopy. Part II. Determination of diffusional pathlengths in synthetic membranes and human stratum corneum. Int J Pharm, 154:217–27.
16. Brancaleon L, Bamberg MP, Sakamaki T, Kollias N. (2001). ATR-FTIR spectroscopy as a possible method to investigate biophysical parameters of stratum corneum *in vivo*. J Invest Dermatol, 116:380–86.
17. Ding PT, Hao JS, Zheng JM. (2000). The study of the mechanism of two enhancers in human *in vivo* by ATR-FTIR. Acta Biophysica Sinica, 16:48–52.
18. Potts RO, Guzek DB, Harris RR, McKie JE. (1985). A noninvasive, in vivo technique to quantitatively measure water concentration of the stratum conrneum using attenuated total reflectance infrared spectroscopy. Arch Dermatol Res, 277:489–95.
19. Obata Y, Utsumi S, Watanabe H, Suda M, Tokudome Y, Otsuka M, et al. (2010). Infrared spectroscopic study of lipid interaction in stratum corneum treated with transdermal absorption enhancers. Int J Pharm, 389:18–23.
20. Kligman AM, Christophers E. (1963). Preparation of isolated sheets of human stratum corneum. Arch Dermatol, 88:70–73.
21. Fang L, Kobayashi Y, Numajiri S, Kobayashi D, Sugibayashi K, Morimoto Y. (2002). The enhancing effect of a triethanolamine – ethanol–isopropyl myristate mixed system on the skin permeation of acidic drugs. Biol Pharm Bull, 25:1339–44.
22. Niazy EM. (1996). Differences in penetration-enhancing effect of Azone through excised rabbit, rat, hairless mouse, guinea pig and human skins. Int J Pharm, 130:225–30.
23. Scheuplein RJ. (1978). Site variations in diffusion and permeability. In: Jarret A, ed. The physiology and pathophysiology of skin. New York: Academic Press, 1693–1730.
24. Lee PJ, Ahmad N, Langer R, Mitragotri S, Shastri VP. (2006). Evaluation of chemical enhancers in the transdermal delivery of lidocaine. Int J Pharm, 308:33–39.
25. Leichtnam ML, Rolland H, Wüthrich P, Guy RH. (2006). Identification of penetration enhancers for testosterone transdermal delivery from spray formulations. J Control Release, 113:57–62.
26. Yamashita F, Bando M, Koyama Y, Kitagawa SM, Takakura. Y, Hashida M. (1994). *In vitro* and *in vivo* analysis of skin penetration enhancement based on a two-layer diffusion model with polar and nonpolar routes in the stratum corneum. Pharm Res, 11:185–91.
27. Yamashita F, Koyama Y, Kitano M, Takakura Y, Hashida M. (1995). Analysis of *in vivo* skin penetration enhancement by oleic acid based on a two-layer diffusion model with polar and nonpolar routes in the stratum corneum. Int J Pharm, 117:173–79.
28. Golden GM, Mckie JE, Potts RO. (1987). Role of stratum corneum lipid fluidity in transdermal drug flux. J Pharm Sci, 76:25–28.
29. Pilgram GS, VanPelt AM, Spies F, Bouwstra JA, Koerten HK. (1998). Cryo-electron diffraction as a tool to study local variations in the lipid organization of human stratum corneum. J Microsc, 189:1–78.
30. Sweeny TM, Downing DT. (1970). The role of the lipids in the epidermal barrier to water diffusion. J Invest Dermatol, 55:135–40.
31. Sato K, Sugibayashi K, Morimoto Y. (1988). Effect and mode of acion of aliphatic esters on the *in vitro* skin permeation of nicorandil. Int J Pharm, 43:31–40.
32. Stroppolo D, Bonadeo M, Chiodo L, Soldati A, Gazzaniga F. (1991). *In vitro* percutaneous penetration of the β2-agonist, broxaterol: Influence of several enhancers. In: Scottt RC, Guy RH, Hadgraft J., Bodde HE, eds. Prediction of percutaneous penetration: Methods; measurements modelling. London: IBC Technical Services Ltd., 373–379.
33. Cettina MG, Liu P, Nightingale J, Bergstrom TK. (1995). Enhanced transdermal delivery of estradiol *in vitro* using binary vehicles of isopropyl myristate and short-chain alkanols. Int J Pharm, 114:237–45.
34. Fang C, Liu Y, Ye X, Rong Z, Feng X, Jiang C, et al. (2008). Synergistically enhanced transdermal permeation and topical analgesia of tetracaine gel containing menthol and ethanol in experimental and clinical studies. Eur J Pharm Biopharm, 68:735–40.
35. Fang L, Numajiri S, Kobayashi D, Morimoto Y. (2003). The use of complexation with alkanolamines to facilitate skin permeation of mefenamic acid. Int J Pharm, 262:13–22.
36. Lin SY, Duan KJ, Lin TC. (1996b). Simultaneous determination of the protein conversion process in porcine stratum corneum after pre-treatment with skin enhancers by a combined microscopic FT-IR/DSC system. Spectrochim Acta A, 52:1671–78.
37. Dubey V, Mishra D, Jain NK. (2007). Melatonin loaded ethanolic liposomes: Physicochemical characterization and enhanced transdermal delivery. Eur J Pharm Biopharm, 67:398–405.
38. Dreher F, Walde R, Walther R, Wehrli E. (1997). Interaction of a lecithin microemulsion gel with human stratum corneum and its effect on transdermal transport. J Control Release, 45:131–40.
39. Vitoria M, Bentley LB, Kedor ERM, Vianna RF, Collett JH. (1997). The influence of lecithin and urea on the *in vitro* permeation of hydrocortisone acetate through skin from hairless mouse. Int J Pharm, 146:255–62.
40. Zbytovska J, Raudenkolb S, Wartewig S. (2004). Phase behavior of transkarbam 12. Chem Phys Lipids, 129:97–109.
41. Kaidi Z, Jagdish S. (1998). Mechanisms of percutaneous absorption of tamoxifen by terpenes: Eugenol, D-limonene and menthone. J Control Release, 55:253–60.
42. Gooris GS, Bouwstra JA. (2007). Infrared spectroscopic study of stratum corneum model membranes prepared from human ceramide, cholesterol and fatty acids. Biophys J, 92:2785–95.
43. Narishetty STK, Panchagnula R. (2004). Transdermal delivery of zidovudine: Effect of terpenes and their mechanism of action. J Control Release, 95:367–79.
44. Potts RO, Francoeur ML. (1993). Infrared spectroscopy of stratum corneum lipids: *In vitro* results and their relevance to permeability. In: Walters KA ., Hadgraft J, eds. Pharmaceutical skin permeation enhancement. New York: Marcel Dekker, 269–291.
45. Rerek ME, Van WD, Mendelsohn R, Moore DJ. (2005). FTIR spectroscopic studies of lipid dynamics in phytosphingosine ceramide model of the stratum corneum lipid matrix. Chem Phys Lipids, 134:51–58.

46. Casal HL, Mantsch HH. (1984). Polymorphic phase behaviour of phospholipid membranes studied by infrared spectroscopy. Biochim Biophys Acta, 779:381–401.
47. Bhatia KS, Singh J. (1998). Mechanism of transport enhancement of LHRH through porcine epidermis by terpenes and iontophoresis: Permeability and lipid extraction studies. Pharm Res, 15:1857–62.
48. Takahashi K, Sakano H, Yoshida M, Numata N, Mizuno N. (2001). Characterization of the influence of polyol fatty acid esters on the permeation of diclofenac through rat skin. J Control Release, 73:351–58.
49. Yokomizo Y, Sagitani H. (1996). Effects of phospholipids on the *in vitro* percutaneous penetration of prednisolone and analysis of mechanism by using attenuated total reflectance-Fourier transform infrared spectroscopy. J Pharm Sci, 85:1220–26.
50. Anigbogu ANC, Williams AC, Barry BW, Edwards HGM. (1995). Fourier transform raman spectroscopy of interactions between the penetration enhancer dimethyl sulfoxide and human stratum corneum. Int J Pharm, 125:265–82.
51. Ayala-Bravo HA, Quintanar-Guerrero D, Naik A, Kalia YN, Cornejo-Bravo JM, Ganem-Quintanar A. (2003). Effects of sucrose oleate and sucrose laureate on *in vivo* human stratum corneum permeability. Pharm Res, 8:1267–73.
52. Lin SY, Duan KJ, Lin TC. (1996a). Microscopic FT-IR/DSC system used to simultaneously investigate the conversion process of protein structure in porcine stratum corneum after pretreatment with skin penetration enhancers. Methods Find Exp Clin Pharmacol, 18:175–81.
53. Tu AT. (1982). Raman spectroscopy in biology: Principles and applications. New York: Wiley, 187–233.